

# Critical phenomena at edges and corners<sup>\*</sup>

M. Pleimling and W. Selke<sup>a</sup>

Institut für Theoretische Physik, Technische Hochschule, 52056 Aachen, Germany

Received: 29 January 1998 / Accepted: 17 March 1998

**Abstract.** Using Monte-Carlo techniques, the critical behaviour at edges and corners of the three-dimensional Ising model is studied. In particular, the critical exponent  $\beta_2$  of the local magnetization at edges formed by two intersecting free surfaces is estimated to be, as a function of the opening angle  $\theta$ ,  $0.96 \pm 0.02$  for  $\theta = 135^\circ$ ,  $1.28 \pm 0.04$  for  $90^\circ$ , and  $2.30 \pm 0.10$  for  $45^\circ$ . The critical exponent  $\beta_3$  of the corner magnetization of a cube is found to be  $1.86 \pm 0.06$ . The Monte-Carlo estimates are compared to results of mean field theory, renormalization group calculations and high temperature series expansions.

**PACS.** 05.50.+q Lattice theory and statistics; Ising problems – 68.35.Rh Phase transitions and critical phenomena – 75.40.Mg Numerical simulation studies

## 1 Introduction

Critical phenomena may be associated not only with the bulk of a three-dimensional crystal, but also with its surfaces, edges and corners. The critical properties of perfect, flat surfaces have been studied extensively [1–3].

However, the singularities of edge and corner quantities have attracted less attention. Some years ago, Cardy noted and calculated the dependence of the edge critical exponents on the opening angle  $\theta$  between the surfaces forming the edge (or wedge), using mean field theory and renormalization group theory of first order in  $\epsilon$  for  $O(n)$  models [4]. Most of the later work dealt with Ising models in two dimensions [5] or polymers [6]. Rather rarely, the critical behaviour of edges in three-dimensional Ising models (describing magnetic crystals or lattice gas systems such as alloys) has been studied, applying renormalization group theory or high temperature series expansions [7–9]. Likewise, the singular properties at the corners of three-dimensional systems has been investigated even only in the framework of mean field theory [5].

Edges and corners may be expected to play a dominant role, for instance, in nanostructured materials. Recently, many studies have been performed to reproduce theoretically properties of such small clusters of atoms, including several Monte-Carlo simulations [10, 11]. In that context, it looks worthwhile to study systematically various types of edges and corners in somewhat simplified models, as well, as will be presented in this article.

The outline of the article is as follows. In the next section, we shall consider three-dimensional Ising models with different opening angles,  $\theta$ , at the edges. In particular, the critical exponent,  $\beta_2$ , of the edge magnetization

is estimated, based on Monte-Carlo (MC) data obtained from a cluster-flip algorithm. The values for  $\beta_2(\theta)$  are compared to previous results. In Section 3, we shall present our Monte-Carlo findings on Ising cubes, calculating especially the corner magnetization and its critical exponent  $\beta_3$ . Difficulties in extracting the bulk critical exponent from the total magnetization of the cubes are pointed out. A brief summary concludes the article.

## 2 Edges with different opening angles

We consider nearest-neighbour Ising models on simple cubic lattices with ferromagnetic interactions,  $J > 0$ . The Hamiltonian is given by

$$H = - \sum_{(i,j)} J S_i S_j \quad (1)$$

where the sum runs over all bonds  $(i, j)$  between spins,  $S_i = \pm 1$ , at neighbouring sites  $i = (x, y, z)$  and  $j$ . In the thermodynamic limit, the systems display a phase transition with the magnetization  $\langle S_{xyz} \rangle$  vanishing above the critical point. From numerical analyses, the critical temperature,  $T_c$ , is known very accurately,  $k_B T_c = 4.511.. J$  [12, 13].

To introduce edges in Ising magnets, we apply periodic boundary conditions along the, say,  $z$ -axis. The remaining four free surfaces of the crystal may be oriented in various ways leading to different opening angles  $\theta$  at the edges. In particular, for pairs of (100) and (010) surfaces, the opening angle is  $\theta = 90^\circ$ , and the system contains four equivalent edges; case (a) in the following (see Fig. 1). Obviously, the opening angle is invariant against rotating the crystal about the  $z$ -axis. However, for instance,

<sup>\*</sup> Dedicated to J. Zittartz on the occasion of his 60th birthday

<sup>a</sup> e-mail: selke@physik.rwth-aachen.de

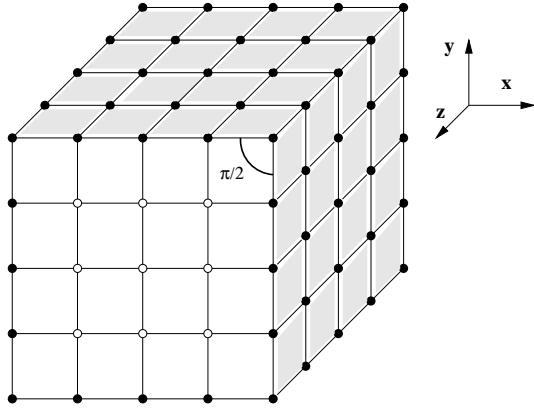


**Fig. 1.** Geometry of an Ising model with (100) and (010) surfaces (shadowed), *i.e.* edges with opening angle  $\theta = 90^\circ$ .

the coordination numbers at the edges may change under a rotation, and therefore the local thermal edge properties may change. Keeping  $\theta = 90^\circ$ , we rotated the crystal by  $45^\circ$  (yielding (110) and  $(1\bar{1}0)$  free surfaces), in order to check whether the critical behaviour at the edges is affected, case (b). In case (c), the surface orientations were chosen to be (100) and (110), with the intersections forming two pairs of edges with  $\theta = 45^\circ$  and  $\theta = 135^\circ$ . Note that edges with an opening angle of  $180^\circ$  correspond to the free surface, whose critical properties have been investigated rather extensively before [1, 2, 14, 15].

In our present Monte-Carlo study of Ising magnets with edges, we used the one-cluster-flip algorithm [16]. Systems with  $L \times M \times N$  sites (or spins) were considered, with  $L \times M$  being the number of sites in the planes perpendicular to the  $z$ -axis, and  $N$  being the number of sites along that axis. Typically,  $L = M$  ranged from 20 to 60, with  $N$  going up to 640. The concrete values were chosen so that finite-size effects could be monitored and avoided, when attempting to elucidate critical properties of indefinitely extended edges, with the bulk and surface properties being those of the thermodynamic limit (see below). Usually,  $4 \times 10^4$  clusters were generated per MC run, discarding the first  $10^4$  clusters for equilibration. We averaged over an ensemble of at least five runs (using different random numbers) to obtain the final thermal averages.

The exchange couplings are assumed to have always the same value,  $J > 0$ , *i.e.* in the bulk as well as at the surfaces and the edges. In the language of surface critical phenomena [1, 2], one then encounters an ordinary transition, with the bulk, surfaces and edges ordering at the same (bulk) critical point,  $T_c$ . Because one expects universal critical behaviour at the ordinary transition, that choice of couplings is merely for reasons of convenience. To cross over to different universality classes (corresponding to the special point or the extraordinary and surface transitions), the surface couplings had to be increased significantly [1, 2, 14, 15].

The crucial quantity of our analysis is the edge magnetization

$$m_2 = \frac{1}{N} \left\langle \left| \sum_z S_{x_0 y_0 z} \right| \right\rangle \quad (2)$$

where  $(x_0 y_0 z)$  denotes a site at an edge of the lattice (in our notation, we follow Cardy [4], using the index “2” to indicate that an edge is formed by the intersection of two planes). In addition, we computed the analogous magnetization for lines parallel to the  $z$ -axis,  $m_l(x, y)$ , as well as the susceptibility,  $\chi_2$ , describing the response of the magnetization to a bulk field [4].

On approach to the bulk critical point,  $T_c$ ,  $m_2$  is expected to vanish as  $m_2 \propto t^{\beta_2}$ , where  $t$  is the reduced temperature,  $t = |T_c - T|/T_c$ . To determine  $\beta_2(\theta)$ , we define, below and at the critical point, an effective exponent [14] as

$$\beta_{2, \text{eff}}(t) = d \ln(m_2) / d \ln(t). \quad (3)$$

Because the MC data are recorded at discrete temperatures,  $t_i$ ,  $\beta_{2, \text{eff}}$  may be determined numerically by

$$\beta_{2, \text{eff}}(t) = \ln(m(z, t_i) / m(z, t_{i+1})) / \ln(t_i / t_{i+1}) \quad (4)$$

with  $t = (t_i + t_{i+1})/2$ .

$\beta_{2, \text{eff}}$  is well defined at all temperatures, not merely close to  $T_c$  (for a related recent study of the corresponding critical exponent near criticality for ferromagnetic thin films, see Ref. [17]). Obviously, when  $t \rightarrow 0$ ,  $\beta_{2, \text{eff}}$  becomes the asymptotic critical exponent  $\beta_2$ . In complete analogy, one may define the effective exponent of the line magnetization,  $m_l$ . For sufficiently large systems,  $m_l$  approaches deep in the interior the bulk magnetization,  $m_b$ , with the corresponding critical exponent  $\beta_b \approx 0.32$  [12, 13]. At the surfaces, far from the edges,  $m_l$  approaches the surface magnetization,  $m_1$ , with the asymptotic critical exponent being  $\beta_1 \approx 0.80$  [14].

To estimate reliably  $\beta_2$  from the simulational data, finite-size effects have to be monitored carefully. Strictly speaking,  $\beta_2$  is defined in the thermodynamic limit,  $L, M, N \rightarrow \infty$  (note that we take the absolute value to define the edge magnetization  $m_2$  in (2), because we are simulating finite lattices). Of course,  $m_2$  is affected by spin fluctuations in the bulk and at the surfaces. Accordingly, the MC system should be large enough to reproduce the thermodynamic values of  $m_b$  and  $m_1$ , sufficiently far away from the edge (these values are known very accurately [12–15]). In general, at a given temperature and geometry of the crystal,  $m_2$  has to be stable against enlarging the system size,  $L \times M$  and  $N$ .

In Figure 2, the finite-size effect is illustrated for the geometry of case (c), with  $\theta = 45^\circ$  and  $135^\circ$ , by plotting  $\beta_{2, \text{eff}}$  versus the reduced temperature (error bars, resulting from ensemble averaging, were determined in the same way as before [14]). Finite-size dependences, *i.e.* deviations from the thermodynamic behaviour, are clearly signalled by a decrease of  $\beta_{2, \text{eff}}$  on approach to  $T_c$ . The crucial quantity is evidently the length of the edge,

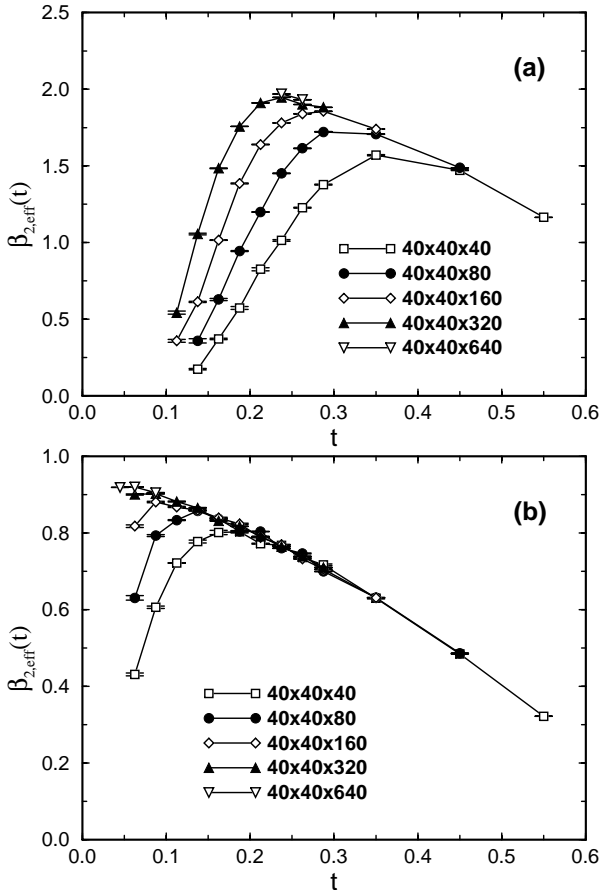


**Fig. 2.** Effective exponent  $\beta_{2,eff}$  of the edge magnetization versus reduced temperature,  $t$ , at edges with opening angles  $\theta =$  (a)  $45^\circ$  and (b)  $135^\circ$ , simulating different sizes  $L \times M \times N$ , see inset.

$N$  (in the range of temperatures depicted in the figure, the size of the planes perpendicular to the  $z$ -axis is sufficiently large,  $L = M = 40$ , to neglect further finite-size dependences, as we checked). By comparing our MC data for  $\theta = 45^\circ, 90^\circ, 135^\circ$ , and  $180^\circ$  (free surface), an increasing edge length is needed to circumvent finite-size effects at fixed temperature and decreasing opening angle.

This trend may be understood by presuming that the critical behaviour at the edges is mainly governed by bulk critical fluctuations, similar to the situation at surfaces [14,15]. Now, by lowering  $\theta$ , less paths between neighbouring spins or sites connect the edges and the bulk. Accordingly, the edge length has to be enlarged to ‘transmit’ the bulk fluctuations fully to the edges at that reduced connectivity.

It would be of interest to establish the finite-size scaling form of the edge magnetization  $m_2(t, L = M, N)$  or, more generally, of the line magnetization  $m_l(\mathbf{d}, t, L = M, N)$ , where  $\mathbf{d}$  denotes the distance of the line to the edge. However, such analyses are beyond the scope of this article. It seems worth mentioning that our MC data suggest that the profile  $m_l(\mathbf{d})$  approaches the surface magnetization,  $m_1$ , or the bulk magnetization,  $m_b$ , along, *e.g.*,

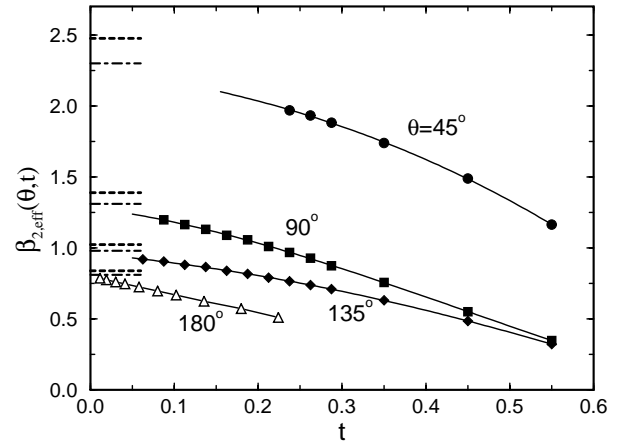


**Fig. 3.**  $\beta_{2,eff}$  versus  $t$  at edges with opening angles  $\theta = 180^\circ$  (triangles) [14],  $135^\circ$  (diamonds),  $90^\circ$  (squares), and  $45^\circ$  (circles). MC system sizes were chosen to circumvent finite-size effects, see text. The predictions of RNG calculations (dashed line) [4] and HTS expansions (dot-dashed line) [7] for  $\beta_2$  are shown as well.

the shortest paths, in an exponential form, *i.e.*

$$m_{b(1)} - m_l(\mathbf{d}) \propto \exp(-a_{b(1)} |\mathbf{d}|). \quad (5)$$

From a preliminary analysis of our MC data, it seems conceivable that  $a_b$  and  $a_1$  become identical on approach to  $T_c$ , being related to the bulk correlation length. A similar behaviour holds for the magnetization profile as a function of the distance from the surface [14,15,18,19].

Figure 3 summarizes our simulational results for the effective exponent  $\beta_{2,eff}(\theta, t)$  in the cases (a) and (c), *i.e.* with one pair of (100) surfaces. Only those MC data are shown which are not significantly affected by finite-size effects. We also included results of our previous MC study for the surface magnetization [14], corresponding to  $\theta = 180^\circ$ .

The slope of  $\beta_{2,eff}$  changes rather mildly at sufficiently small reduced temperatures  $t$ . Thereby meaningful estimates for the asymptotic exponent  $\beta_2(\theta)$  seem to be feasible, with uncertainties rising when lowering the opening angle, because of a lack of MC data close to criticality due to the stronger finite-size effect. Our estimates are  $\beta_2(\theta = 180^\circ) = 0.80 \pm 0.01$  [14],  $\beta_2(135^\circ) = 0.96 \pm 0.02$ ,  $\beta_2(90^\circ) = 1.28 \pm 0.04$ , and  $\beta_2(45^\circ) = 2.30 \pm 0.10$ , with error bars referring to ‘reasonable’ extrapolations of the effective exponents to the critical point.

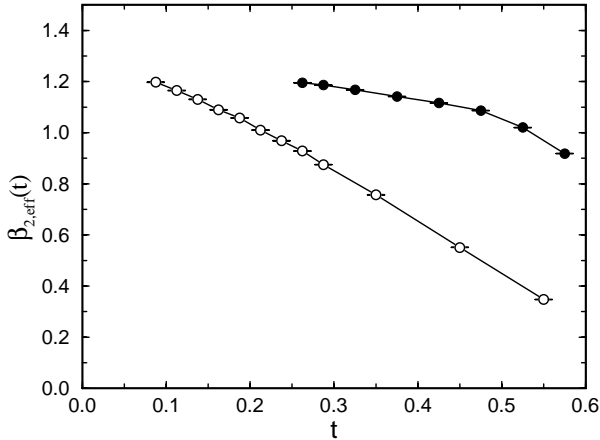
These MC estimates are to be compared with results obtained from mean field theory (MF) [4], renormalization group calculations to first order in  $\epsilon$  (RNG) [4], and high temperature series expansions (HTS) [7], see Figure 3 and Table 1. The values given by mean field theory

$$\beta_2(\theta) = \frac{1}{2} \left( 1 + \frac{180^\circ}{\theta} \right) \quad (6)$$

are presumably systematically too high, according to the predictions of the renormalization group. These predictions, in turn, seem to be systematically too large, as

**Table 1.** Predictions for edge critical exponent  $\beta_2$ , using various methods discussed in the text.

	45°	90°	135°	180°
MF [4]	2.50	1.50	1.17	1.00
RNG [4]	2.48	1.39	1.02	0.84
HTS [7]	2.30	1.31	0.98	0.81
MC	$2.30 \pm 0.10$	$1.28 \pm 0.04$	$0.96 \pm 0.02$	$0.80 \pm 0.01$ [14]

**Fig. 4.**  $\beta_{2,eff}$  versus  $t$  at edges with  $\theta = 90^\circ$ , with pairs of (100) and (010) surfaces (open circles) and pairs of (110) and  $(\bar{1}\bar{1}0)$  surfaces (full circles), for MC system sizes up to  $60 \times 60 \times 640$  to avoid finite-size dependences.

suggested both by high temperature series expansions and the MC simulations. The last two methods yield results which are in close agreement with each other. A similar tendency in the values of  $\beta_2(\theta)$  obtained from the different analytical and numerical approaches (MF, RNG, HTS, and MC) holds for the  $n$ -vector model with  $n = 0$ , describing polymers [4, 7, 20].

At the fixed opening angle  $\theta = 90^\circ$ , we studied the effect of a rotation of the crystal on the critical edge properties, case (b). In particular, the crystal was rotated by  $45^\circ$  about the  $z$ -axis. The wedge is then formed by (110) and  $(\bar{1}\bar{1}0)$  surfaces. By the rotation, the coordination numbers at the surfaces and edges are reduced by one. Consequently, the surface and edge magnetizations are lowered. Following the above considerations, the finite-size effect is expected to be enhanced compared to case (a), *i.e.* after rotation, larger MC systems are needed to approximate closely the thermodynamic behaviour. The MC data confirm this expectation.

Results on the effective exponent  $\beta_{2,eff}$  are displayed in Figure 4, comparing the cases (a) and (b). Again, we depict only MC data which are not significantly affected by finite-size effects. It seems well conceivable to extrapolate both cases to the same asymptotic critical exponent,  $\beta_2 = 1.28 \pm 0.04$ , consistent with the invariance of the value of the boundary critical exponent against rotation of the crystal. After rotation, we did not approach the critical point as closely as before, because otherwise ex-

tremely large systems had to be dealt with. In any event, as seen in Figure 4, corrections to scaling are much weaker in case (b), for small reduced temperatures, resulting in the much lower slope of  $\beta_{2,eff}$ , compared to Ising models with (100) and (010) surfaces.

Note that the invariance of boundary critical exponents against rotation of the crystal has been discussed and partly even proven for surfaces and edges of two-dimensional Ising models [5, 19, 21].

Our MC data for the exponent of the edge susceptibility,  $\chi_2$ , are less accurate than those for the edge magnetization, thereby allowing to estimate the corresponding critical exponent  $\gamma_2$  only with rather large uncertainties. At any rate,  $\gamma_2$  is found to depend strongly on the opening angle  $\theta$ , and the results of the RNG calculations and HTS method [4, 7] seem to provide fairly good estimates for the true values.

### 3 Cubes and corners

We consider Ising cubes of  $L^3$  spins on simple cubic lattices with free surfaces. In the thermodynamic limit,  $L \rightarrow \infty$ , the corner magnetization is given by

$$m_3 = \frac{1}{8} \left\langle \sum_{x_0 y_0 z_0} S_{x_0 y_0 z_0} \right\rangle \quad (7)$$

summing and averaging over the eight corner spins at sites  $(x_0 y_0 z_0)$ . In complete analogy to (3), one may define an effective exponent  $\beta_{3,eff}$ , approaching the asymptotic corner critical exponent  $\beta_3$ , as  $t \rightarrow 0$ .

In a finite system,  $m_3$  is, strictly speaking, zero, because the Hamiltonian is invariant against reversing the spins. On the other hand, for instance, the absolute corner magnetization

$$m_{3,a} = \frac{1}{8} \left\langle \left| \sum_{x_0 y_0 z_0} S_{x_0 y_0 z_0} \right| \right\rangle \quad (8)$$

seems to show no critical behaviour. Indeed,  $m_{3,a}$  is quite distinct from  $m_3$ , involving a fixed number of spins independent of the system size, in contrast to the bulk, surface or edge magnetizations calculated with or without absolute values.

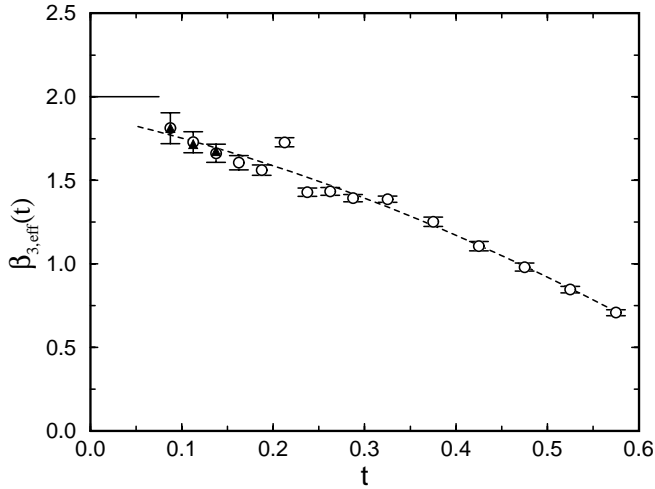


**Fig. 5.** Effective exponent  $\beta_{3,eff}$  of the corner magnetization as a function of  $t$  for Ising cubes with  $20^3$  spins (open circles) and, for comparison at small  $t$ , with  $40^3$  spins (full triangles). The broken line is a guide to the eye. The solid line refers to the value of  $\beta_3$  as calculated from mean field theory [5].

To compute  $m_3$ , we use the standard one-spin-flip MC algorithm (Metropolis algorithm). Taking the fully ordered ground state with, say,  $S_{xyz} = 1$  at all sites as starting configuration of the simulation, one encounters, after initial relaxation, at  $T < T_c$ , a metastable state, in which the total magnetization is positive. The system remains in that metastable state (being separated by an energy barrier from the “mirror” metastable state with negative total magnetization), possibly, for a long time, the time depending on the size  $L$  and the temperature, see, *e.g.*, reference [22]. The corresponding local magnetizations, especially the corner magnetization  $m_3$ , do not vanish then, and their values, taking usual finite-size dependences into account, are supposedly very close to those in the thermodynamic limit.

In fact, by monitoring the total magnetization during the MC runs, we identified the temperatures at which we can reliably compute  $m_3$ . In Figure 5, resulting findings for the effective exponent,  $\beta_{3,eff}$ , are shown. Most of the data are for rather small cubes (mimicking magnetic nanoparticles), with  $L = 20$ . 3000 Monte-Carlo steps per site (MCS) were used to “equilibrate” (to the metastable state) the systems; additional 7000 MCS were performed to obtain thermal averages. To improve the statistics, we sampled over an ensemble of a few  $10^2$  independent MC runs at each temperature. No finite-size effects were observed, when we increased  $L$  to 40 at the smallest reduced temperatures, see Figure 5. To generate data of the high accuracy required to determine reliably the effective exponent without finite-size corrections closer to  $T_c$ , one had to simulate eventually much larger system sizes. In that way, the computing time had to be increased appreciably then. We refrained from doing so, because the present data already allow for a decent estimate of the asymptotic critical exponent,  $\beta_3 = 1.86 \pm 0.06$ . That value is signifi-

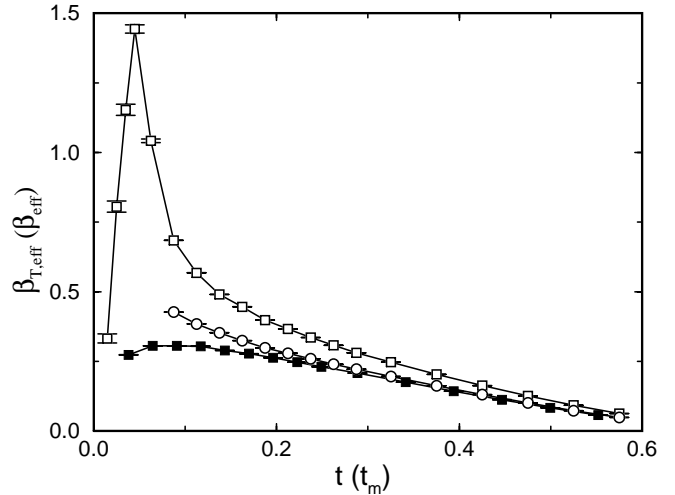


**Fig. 6.** Effective exponent of the total magnetization  $\beta_{T,eff}$  ( $\beta_{eff}$ ; full symbols) versus reduced temperature  $t$  ( $t_m$ ) of an Ising cube with  $20^3$  (squares) and  $40^3$  (circles) spins, using different reference temperatures for the (finite-size) critical point  $T_c$  ( $T_m$ ), see text.

cantly lower than the one predicted by mean field theory,  $\beta_3 = 2$  [5].

In finite-size scaling theories [23,24], one usually considers the total magnetization of the system, summing and averaging over all spins. This approach may work in the simplest form by using periodic boundary conditions, implying translational invariance. Of course, in the case of free surfaces much care is needed, because the contributions of bulk, surface, edge, and corner spins to the total magnetization are of different type. Actually, the local magnetization differs, in general, from site to site.

In Figure 6, the effective exponent,  $\beta_{T,eff}$  of the total magnetization  $m_T$ , taking, in analogy to (2), the absolute values, is shown again for a relatively small cube with  $20^3$  spins (including, for comparison, data for  $L = 40$ ).  $\beta_{T,eff}$  is appreciably higher than the bulk critical exponent  $\beta_b = 0.32$  already quite far away from criticality,  $t < 0.2$ . The “overshooting phenomenon” is caused by the spins near the surfaces, edges and corners, reducing the total magnetization and yielding large effective and critical exponents, as discussed in this article. Certainly, on approach to  $T_c$  the effective exponent goes to zero, because the absolute total magnetization  $m_T$  does not vanish at the critical point in a finite system.

The overshooting persists at larger system sizes (becoming, however, weaker at fixed  $t$ ; see Fig. 6 for  $L = 40$ ), and it may be difficult to extract the correct bulk critical exponent reliably. In an alternate approach, one may replace the reduced temperature  $t$  by  $t_m = |T - T_m|/T_m$ , where  $T_m$  denotes the turning point of the total magnetization for a given system size,  $L$ . From  $\beta_{eff} = d \ln(m_T)/d \ln(t_m)$ , one might estimate  $\beta_b$  (for  $L \rightarrow \infty$  one has  $t_m \rightarrow t$ , and thence  $\beta_{eff} \rightarrow \beta_b$  as  $t \rightarrow 0$ ) in an easy way, see Figure 6. For larger system sizes,  $\beta_{T,eff}$  and  $\beta_{eff}$  tend to approach each other,

as one observes, *e.g.*, for systems with  $L = 40$ . In any event, detailed considerations would be desirable to substantiate and quantify the finite-size effects for Ising cubes (for related problems, demonstrating the sensitivity of finite-size scaling to different boundary conditions, see, *e.g.*, Refs. [23,24]).

## 4 Summary

Using Monte-Carlo techniques, we studied critical properties of edges and corners in three-dimensional Ising models. In particular, by computing effective exponents for the edge and corner magnetization, the corresponding asymptotic critical exponents could be estimated quite reliably.

The critical exponents at the edges are found to depend sensitively on the opening angle formed by the surfaces intersecting at the edge. The numerical values for these exponents, based on the simulational data, refined predictions of renormalization group calculations of first order in  $\epsilon$ , and confirmed results of high temperature series expansions. The exponents seem to be invariant against rotating the crystal, but keeping the opening angle, as we demonstrated in a specific case. However, the corrections to scaling may be largely affected by such a rotation.

The critical exponent at the corner had been calculated before only by using mean field theory. The estimate based on the Monte-Carlo data shows that the true value is significantly lower than the one predicted by mean field theory. It would be interesting to apply other numerical and analytical techniques to determine that exponent.

By simulating corner properties, we considered Ising models on a cube with free surfaces (mimicking magnetic nanoparticles). Such systems show very strong finite size effects, when calculating quantities averaging over the entire lattice. Care is needed in extracting bulk critical properties, because the singularities at the surfaces, edges, and corners are distinct from the bulk singularities, and play an important role even for fairly large system sizes.

We should like to thank H.W. Diehl for suggesting to us to study the edge problem, and F. Iglói for a useful discussion. It is a pleasure, to thank here J. Zittartz for gratifying interactions with one of us (W.S.) during many years in organizing the Landau-Seminars "Cooperative Phenomena in Many-Particle Systems in Physics".

## References

1. K. Binder, in *Phase Transitions and Critical Phenomena*, Vol. 8, edited by C. Domb, J.L. Lebowitz (London, Academic Press, 1983).
2. H.W. Diehl, in *Phase Transitions and Critical Phenomena*, Vol. 10, edited by C. Domb, J.L. Lebowitz (London, Academic Press, 1986); *Int. J. Mod. Phys. B* **11**, 3503 (1997).
3. H. Dosch, *Critical Phenomena at Surfaces and Interfaces* (Berlin, Heidelberg, New York: Springer, 1992).
4. J. Cardy, *J. Phys. A: Math. Gen.* **16**, 3617 (1983).
5. F. Iglói, I. Peschel, L. Turban, *Adv. Phys.* **42**, 683 (1993).
6. K. De Bell, T. Lookman, *Rev. Mod. Phys.* **65**, 87 (1993).
7. A.J. Guttmann, G.M. Torrie, *J. Phys. A: Math. Gen.* **17**, 3539 (1984).
8. Z.-G. Wang, A.M. Nemirovsky, K.F. Freed, K.R. Myers, *J. Phys. A: Math. Gen.* **23**, 2575 (1990).
9. T.A. Larsson, *J. Phys. A: Math. Gen.* **19**, 1691 (1986).
10. J. Merikoski, J. Timonen, M. Manninen, P. Jena, *Phys. Rev. Lett.* **66**, 938 (1991).
11. D.A. Dimitrov, G.M. Wysin, *Phys. Rev. B* **54**, 9237 (1996).
12. A.M. Ferrenberg, D.P. Landau, *Phys. Rev. B* **44**, 5081 (1991).
13. A.L. Talapov, H.W.J. Blöte, *J. Phys. A: Math. Gen.* **29**, 5727 (1996).
14. M. Pleimling, W. Selke, *Eur. Phys. J. B* **1**, 385 (1998).
15. D.P. Landau, K. Binder, *Phys. Rev. B* **41**, 4633 (1990).
16. J.S. Wang, R.H. Swendsen, *Physica A* **167**, 565 (1990); *U. Wolff, Phys. Rev. Lett.* **60**, 1461 (1988).
17. P. Schilbe, K.H. Rieder, *Europhys. Lett.* **41**, 219 (1998).
18. D. Wingert, D. Stauffer, *Physica A* **219**, 135 (1995).
19. W. Selke, F. Szalma, P. Lajko, F. Iglói, *J. Stat. Phys.* **89**, 1079 (1997); F. Iglói, P. Lajko, W. Selke, F. Szalma, *J. Phys. A: Math. Gen.* **31**, 2801 (1998).
20. D.S. Gaunt, S.A. Colby, *J. Stat. Phys.* **58**, 539 (1990).
21. M.N. Barber, I. Peschel, P.A. Pearce, *J. Stat. Phys.* **37**, 497 (1984); I. Peschel, *Phys. Lett. A* **110**, 313 (1985); B. Davies, I. Peschel, *Ann. Physik* **6**, 187 (1997).
22. S. Miyashita, H. Takano, *Prog. Theoret. Phys.* **73**, 1122 (1985).
23. M.N. Barber, in *Phase Transitions and Critical Phenomena*, Vol. 8, edited by C. Domb, J.L. Lebowitz (London: Academic Press, 1983); M.E. Fisher, in: *Critical Phenomena*, Proc. 51st Enrico Fermi Summer School, edited by M.S. Green (New York: Academic Press, 1970).
24. K. Binder, in: *Computational Methods in Field Theory*, edited by H. Gausterer, C.B. Lang (Berlin: Springer, 1992); V. Dohm, *Physica Scripta T* **49**, 46 (1993); S. Dasgupta, D. Stauffer, V. Dohm, *Physica A* **213**, 368 (1995).